

Optimum Design of the Multifacet Drill

T.I. Liu and S.M. Wu

A two-stage strategy has been used to design an optimum multifacet drill (MFD) for crankshaft drilling. In the first stage, a heuristic MFD was developed by adding an additional facet to the outer corner of the conventional split-point drill. Under accelerated life test conditions, this new drill can decrease thrust force by 21.0% and increase drill life by 50% compared to a split-point drill. In the second stage, comprehensive force models for predicting thrust and torque were modified and developed. Using the force models, point optimization was carried out to design the optimum MFD. This new MFD can further decrease the thrust by 21.3% over the heuristic MFD, and accelerated life tests have shown a 25% further increase in drill life.

Keywords

force models, optimum design, thrust and torque

1. Introduction

THE drilling operation is a bottleneck in the manufacturing processes. To improve the quality of drilled holes and increase drill life, attempts have been made to develop new multifacet drills (MFDs), which have been proved to be highly successful.^[1,2,3,4]

In this work, an optimum MFD was designed for crankshaft drilling using a two-stage strategy. This drill can be used to replace the conventional split-point drill that has been used historically to produce small-diameter deep holes in automotive crankshafts.

In the first stage, a heuristic approach was adopted by using information obtained from previous MFDs.^[1,5] Second, force models, particularly those of MFDs, were modified and developed so that an optimization program could be used to design a MFD for crankshafts. The results were verified by drilling experiments.

2. Heuristic Development of the MFD—Design Stage I

A new type of MFD for crankshafts was developed heuristically with the intent of increasing drill life. The approach taken was to reduce thrust by changing the drill point geometry. Past experiences in drilling, and particularly in the design of previous MFDs, contributed to the development of this new MFD.^[1,4]

Since their original development in the 1950s for drilling armor plates, MFDs have been reported to have reduced thrust by 35 to 50% and torque by 10 to 30% compared to a conventional twist drill. MFDs have been able to increase drill life by 300 to 500%. It has also been reported that hole quality and chip-

breaking capability have been greatly improved by use of MFDs.^[4,6]

A trial-and-error approach was taken to design the MFD point geometry, resulting in more than 30 combinations. In grinding MFDs, one cylindrical surface was added to the inner part of the flute of a conventional twist drill, and another was added to its flank. In this manner, the drill center was lowered, two additional sharp points were formed, and the chisel edge length was reduced. These sharp points improved drill centering and chip-breaking capabilities. Also, thrust was decreased because of an increase in the rake angle on the inner part of the cutting edge and a decrease in the chisel edge length. Furthermore, another facet was added to the outer corner of the MFD point to provide a chamfered effect.

The split-point drill has been used in the drilling of crankshafts for many years; however, its performance still needs improvement. For this reason, a heuristic MFD for crankshafts,

Nomenclature	
B =	Chisel edge length
f =	Feed per revolution
H_B =	Workpiece hardness
i =	Inclination angle
M =	Torque
R =	Drill radius
r =	radius to the center of the segment in question
T =	Thrust
α_s =	Side rake angle
α_b =	Back rake angle
α_e =	Effective rake angle
α_D =	Dynamic rake angle
β =	Friction angle
β_1 =	Friction angle of oblique cutting
γ =	Feed angle
V_c =	Cutting speed at the center of each segment in question
$\bar{\gamma}$ =	Average shear strain rate
ψ =	Chisel edge angle
ϕ =	Shear angle
ϕ_1 =	Shear angle of oblique cutting
η =	Chip flow angle
2ϕ =	Point angle of middle cutting edge
$2\phi_1$ =	Point angle of outer cutting edge
$2\phi_2$ =	Point angle of inner cutting edge

T.I. Liu, Department of Mechanical Engineering, California State University, Sacramento, California; and S.M. Wu, Department of Mechanical Engineering and Applied Mechanics, University of Michigan, Ann Arbor, Michigan.

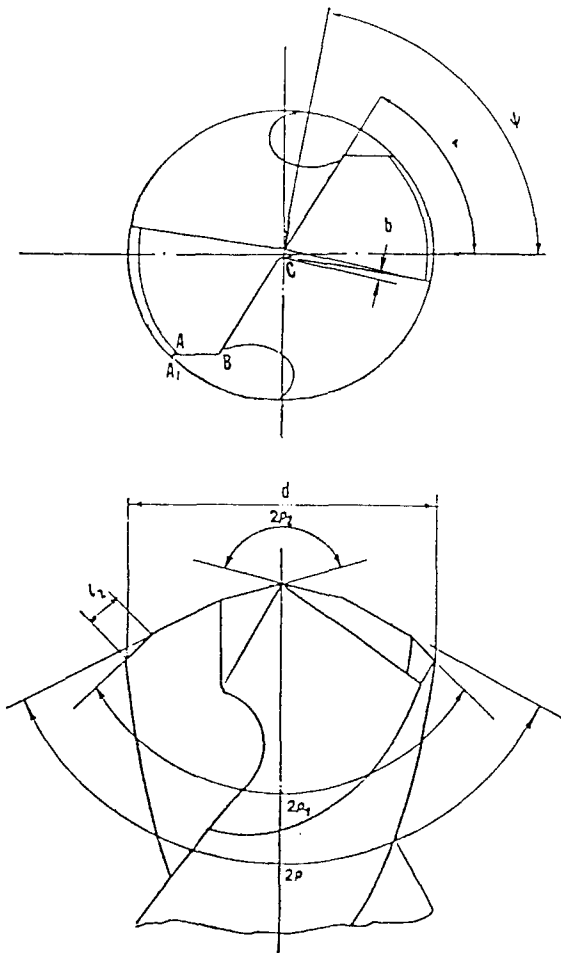


Fig. 1 Configuration of the multifacet drill.

which combines features of previous MFDs and of the split-point drill, was developed. Because the split-point drill currently used in industry has a heavy web, a split point was used to increase the rake angle on the inner cutting edge and reduce the chisel edge length. Another facet was added to the outer corner. Thus, the heuristic MFD has triple point angles, $2p$, $2p_1$, and $2p_2$ (Fig. 1). The thrust can be greatly reduced by using this new point geometry. The performance of the heuristic MFD, in which the thrust, torque, and drill life were evaluated, was compared to that of a split-point drill.

Thrust and torque were used as indexes of drill life. Thrust and torque were measured while drilling 1×0.25 in. (25.4 \times 6.35 mm) breakthrough holes in nodular cast iron workpieces. The entry surface was perpendicular to the drills, and a drill bushing was used. The spindle speed was 2100 rpm and the feedrate was 0.007 ipr (0.178 mm/rev).

The measured thrust and torque of the split-point drill were 266.1 lb (1184 N) and 30.1 lb · in. (340 N · cm), respectively. For the heuristic MFD, the thrust and torque were 210.2 lb (935 N) and 28.9 lb · in. (326 N · cm). Comparing the two, thrust was reduced by 21.0% for the heuristic MFD, whereas torque exhibited a slight decrease.

Although accelerated life testing can only give an indication of the drill performance, it still offers a direction for further in-

vestigation. Therefore, accelerated life tests were carried out to compare the performances of the split-point drill and the heuristic MFD. The spindle speed was 2100 rpm, and the feedrate was 0.007 ipr (0.178 mm/rev). The split-point drills produced only two oil holes in two different drilling tests. Under the same conditions, the heuristic MFDs produced three and four oil holes, an increase of at least 50%.

3. Development of Force Models for the MFD—Basis of Optimum Design

Force models for conventional twist drills have been established for many years. Significant contributions were made by Williams,^[7] in whose model the total thrust and torque, due to the main cutting edges and the chisel edge, were analyzed. Constant shear stress factors were used; however, the effect of feed motion was not considered, and an orthogonal cutting model was assumed.

In a state-of-the-art force model developed for MFDs, Lee^[3] incorporated the effects of dynamic angles. Constant shear stress factors were assumed for all of the cutting edges. An oblique cutting model was used for the main cutting edges. Furthermore, Fuh^[2] pointed out different shear stress factors should be used for different regions of the MFDs.

To develop a new optimum MFD, thrust and torque were selected as criteria to be minimized. Hence, force models for the crankshaft MFD were needed to serve as a basis for its optimization.

In force models for the crankshaft MFDs, the thrust and torque on the main cutting edges and the chisel edge were analyzed separately. The chisel edge length is very small for crankshaft MFDs (only 0.005 in.); therefore, an indentation model was used to simulate its extrusion. Because the crankshaft MFDs have three different cutting edges, different shear stress factors were used for the different cutting edges.

The shear stress factors for different cutting edges of the MFDs were determined experimentally by measuring the thrust and torque on each cutting edge and applying regression analysis. In other words, these factors are empirical coefficients. The developed force models are capable of predicting thrust and torque values under different drilling conditions. Finally, optimization of the MFD point was carried out by using the developed force models.

3.1 Force Contributions of the Main Cutting Edges

For the crankshaft MFD, the main cutting edges consist of the inner, middle, and outer cutting edges. If the main cutting edges are divided into small segments, then each segment is considered as a single-point tool with dynamic rake angle α_D .

The tangential, normal, and side forces for each sliced element, ΔL , of the main cutting edges are denoted as ΔF_t , ΔF_n , and ΔF_s , respectively. They are generated by rotating a feed angle, γ (Fig. 2). Therefore, the force components can be found by adding the feed angle to William's model.^[2,3,8]

$$\Delta F_t = \frac{t_1 \Delta L C_{ij}}{\sin \phi_i \cos (\phi_i + \beta_i - \alpha_D)} \cos (\beta_i - \alpha_D + \gamma) \quad [1]$$

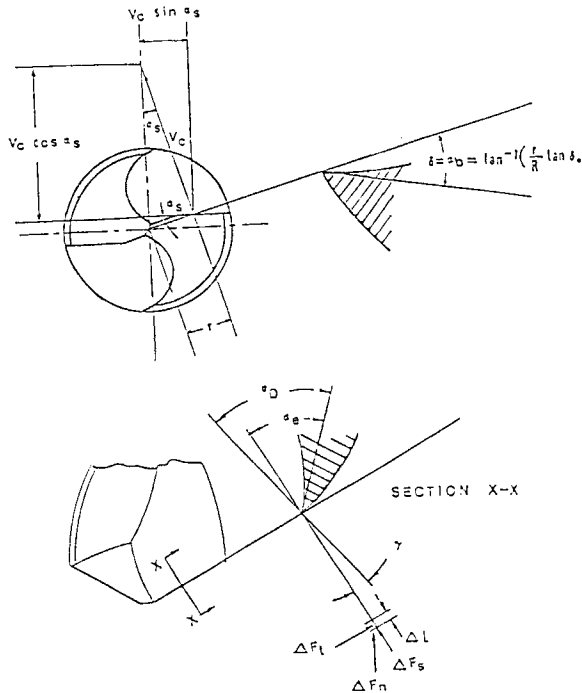


Fig. 2 Dynamic geometry of the cutting edge of the crankshaft multifacet drill.

$$\Delta F_n = \Delta F_t \tan (\beta_i - \alpha_D + \gamma) \quad [2]$$

$$\Delta F_s = \sqrt{\Delta F_t^2 + \Delta F_n^2} \sin \beta_i \tan \eta \quad [3]$$

where C_{ij} 's are the shear stress factors for the main cutting edges; η (chip flow angle) = $\tan^{-1}(\tan i \cos \alpha_D)$; and $t_1 = f \sin(\text{point angle on portion in question}/2) \cos \gamma/2$.

The thrust, $T_L^{(1)}$, and torque, $M_L^{(1)}$, of the inner cutting edge are the integral of the thrust and torque of each segment, as shown in the following equations:

$$T_L^{(1)} = 2 \left(\int_B^C \sin \rho_2 \Delta F_n + \int_B^C \cos \rho_2 \Delta F_s \right) \quad [4]$$

$$M_L^{(1)} = 2 \left(\int_B^C r \cos i \Delta F_t + \int_B^C r \sin i \sin \rho_2 \Delta F_s \right) \quad [5]$$

The thrust, $T_L^{(2)}$, and torque, $M_L^{(2)}$, of the middle cutting edge are:

$$T_L^{(2)} = 2 \left(\int_A^B \sin \rho \Delta F_n + \int_A^B \cos \rho \Delta F_s \right) \quad [6]$$

$$M_L^{(2)} = 2 \left(\int_A^B r \cos i \Delta F_t + \int_A^B r \sin i \sin \rho \Delta F_s \right) \quad [7]$$

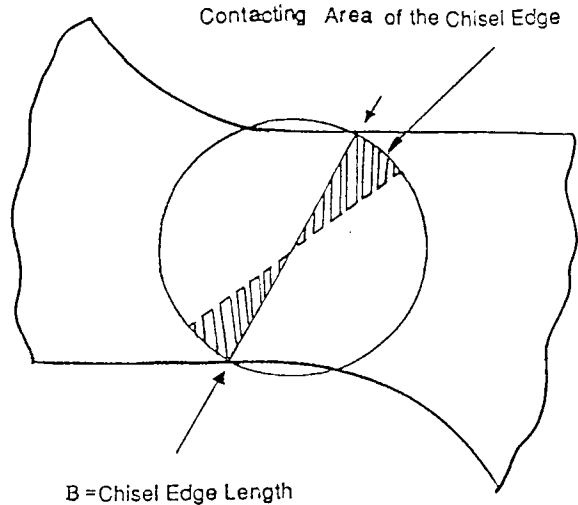


Fig. 3 Indentation model of the chisel edge of the crankshaft multifacet drill.

Similarly, the thrust, $T_L^{(3)}$, and torque, $M_L^{(3)}$, of the outer cutting edge are:

$$T_L^{(3)} = 2 \left(\int_{A_1}^A \sin \rho_1 \Delta F_n + \int_{A_1}^A \cos \rho_1 \Delta F_s \right) \quad [8]$$

$$M_L^{(3)} = 2 \left(\int_{A_1}^A r \cos i \Delta F_t + \int_{A_1}^A r \sin i \sin \rho_1 \Delta F_s \right) \quad [9]$$

3.2 Force Contribution of the Chisel Edge

The chisel edge of the crankshaft MFD can be treated as the central portion of the chisel edge of a conventional twist drill. Lee considered the indentation action as cutting with two side rake angles.^[3]

In this research, the indentation process is modeled as a wedge with a contacting area of 10% of a circle, whose diameter equals the chisel edge length (Fig. 3). Thus, the thrust can be calculated by:

$$T_c = 0.1 \left(\frac{\pi B^2}{4} \right) H_B \quad [10]$$

where B is the chisel edge length; and H_B is the Brinell hardness of the workpiece. The torque on the chisel edge is negligible.

3.3 Total Thrust and Torque

The total thrust (T) and torque (M) are predicted by summing the individual contributions of the inner, middle, and outer cutting edges and chisel edge:

$$T = T_L^{(1)} + T_L^{(2)} + T_L^{(3)} + T_c \quad [11]$$

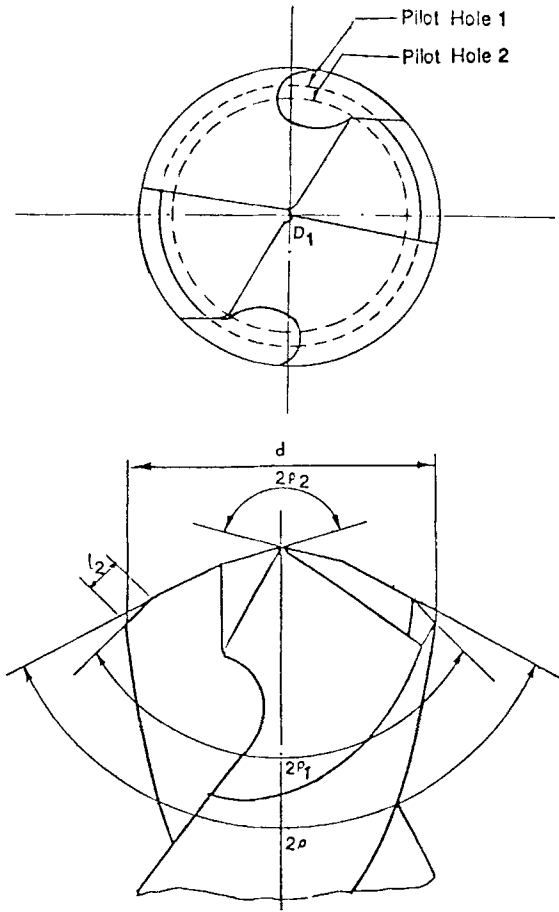


Fig. 4 Different sizes of pilot holes.

$$M = M_L^{(1)} + M_L^{(2)} + M_L^{(3)} \quad [12]$$

3.4 Derivation of the Friction and Shear Angles

The dynamic rake angle, α_D , and the velocity vary in magnitude along the main cutting edges, from the outer periphery to the chisel edge corner. The shear angle is a function of the dynamic rake angle and the friction angle, and the friction angle is a function of the dynamic rake angle.^[2,7,9]

The shear angle, φ , for the model can be expressed as:

$$\varphi = A \alpha_D + B \beta + C \quad [13]$$

and the friction angle, β , can be written as:

$$\beta = D \alpha_D + E \quad [14]$$

where A, B, C, D , and E are constants to be determined.

From the experimental data, the above constants can be determined:^[5,10]

$$\beta = 0.790 \alpha_D + 0.460 \quad [15]$$

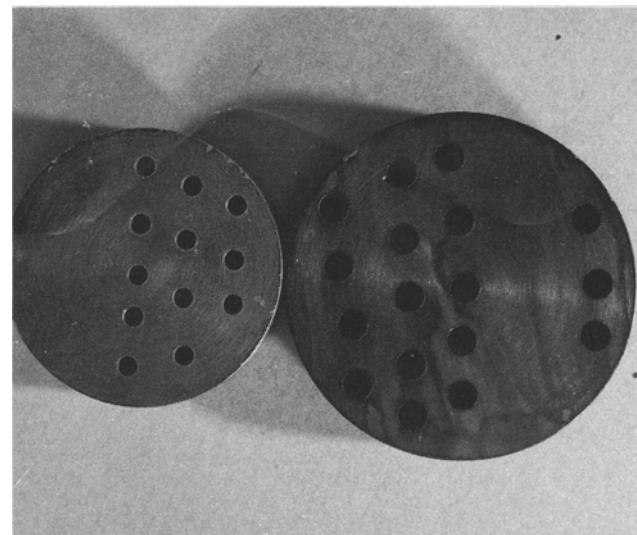


Fig. 5 Photograph of different sizes of pilot holes.

$$\varphi = 0.568 + 0.344 \alpha_D - 0.039 \beta \quad [16]$$

3.5 Prediction of the Thrust and Torque

In the models of chip formation, it is reasonable to assume, on the basis of the work by Oxley,^[11,12] that C_{ij} is a function of the mean shear strain rate, $\bar{\gamma}$, for a particular cutting segment. The values of C_{ij} can be expressed as:

$$C_{ij} = K_{ij} \log \bar{\gamma} + h_{ij} \quad [17]$$

$$i = 1, 2, 3$$

$$j = 1, 2$$

where k_{ij} and h_{ij} are constants to be determined. The mean shear strain rate in this model can be shown as:

$$\bar{\gamma} = \frac{2 V_c \cos \alpha_D \sin \varphi_i}{t_1 \cos (\varphi_i - \alpha_D)} \quad [18]$$

where V_c is the cutting speed (ft/min). The shear stress factors vary with cutting speed and feedrate (Eq 17 and 18).

In Eq 4 through 9, the force contributions of the cutting edges are functions of the ΔF_r , ΔF_n , ΔF_s , and other parameters related to the point geometry and cutting conditions. ΔF_r , ΔF_n , and ΔF_s depend on shear stress factors, C_{ij} , and other parameters, as shown in Eq 1 to 3. To obtain these C_{ij} values, experiments were carried out under different cutting conditions. In these experiments, the force contributions, $T_L^{(i)}$ and $M_L^{(i)}$, were measured. Therefore, in Eq 1 through 9, C_{ij} values are the only unknowns to be determined by regression analysis, because all other parameters can be derived from the point geometry and cutting conditions.

In this study, drilling experiments under three different feedrates, 0.011, 0.007, and 0.004 ipr (0.279, 0.178, and 0.102

mm/rev), and four different spindle speeds, 2100, 1540, 1130, and 830 rpm, were carried out. Thrust and torque were measured. Drilling tests were performed with and without pilot holes. Two different sizes of pilot holes are illustrated in Fig. 4, with Fig. 5 showing the actual holes. The shear stress factors, which are empirical coefficients of force models, were obtained for different cutting edges by using a computer program. Drilling thrust and torque can be estimated using force models after shear stress factors have been obtained empirically.

Additional experiments were performed to verify the developed force models. In different drilling test runs, the experimental data were within 20% of the thrust and torque values estimated by the force models.

4. Optimum Design of the MFD—Design Stage II

To further improve the performance of the heuristic MFD, optimization of the point geometry of the crankshaft MFD was undertaken using a computer program. For crankshaft MFDs, thrust changes significantly when the point geometry is altered. Hence, thrust is a good index of drill performance. Torque of crankshaft MFDs, on the other hand, does not change much when the MFD point geometry changes, as pointed out in Ref 5. However, torque must still be considered, because it also contributes to drill failure. The dimensionless objective function, $J(X)$, is defined using weight factors so that both thrust and torque are taken into account in the point optimization:

$$\begin{aligned} J(X) &= \text{Dimensionless objective function} \\ &= aT + bM \end{aligned}$$

The weight factors, a and b , take care of different units of thrust and torque so as to make the objective function dimensionless. Infinite combinations of values of a and b exist. In this design, the main objective was to minimize thrust. Because the magnitude of the thrust is much larger than that of the torque, the weight factors were chosen to be 1 in this work. A computer program was used to minimize the dimensionless objective function, i.e., $J^* = \min J(X)$.

4.1 Selection of Design Variables

Geometric parameters, such as drill diameter, clearance diameter, land width, web thickness, and the helix angle, cannot be controlled through a point grinding operation and were treated as pre-assigned parameters.

Chisel edge length, B , nominal relief angle, ζ , point angle of the inner cutting edge, $2\varphi_2$, point angle of the middle cutting edge, 2φ , and the point angle of the outer cutting edge, $2\varphi_1$, can be controlled through point grinding operations and are therefore candidates for design variables.

The influence of these five variables on the objective function was obtained by using the developed force models. Usually, chisel edge length does affect thrust force. However, chisel edge length of the crankshaft MFD is small (only 0.005 in., i.e., 0.127 mm) and does not significantly help to reduce the value of the objective function. The chisel edge of the crankshaft MFD can be treated as the central portion of the chisel

Table 1 Constraints of design variables

Design variable	Point angle of outer cutting edge	Point angle of middle cutting edge	Point angle of inner cutting edge
Upper limit (X_{iU})...	90°	120°	150°
Lower limit (X_{iL})...	60°	90°	120°

edge of a conventional twist drill. Wiriyacosol and Armarego even neglected the contribution of this portion to the total thrust and torque in their research on the twist drill.^[13] Hence, chisel edge length was kept constant in this analysis.

The nominal relief angle has no influence on the formulated objective function according to the force models. This simulation result is in agreement with previous research results of other drill geometries.^[14,15] Thus, the nominal relief angle was also kept constant.

The influence of the three point angles, 2φ , $2\varphi_1$, and $2\varphi_2$, on the objective function is significant. When these three angles change, the value of the objective function varies greatly. Therefore, they were selected as design variables. In other words:

$$X = [2\varphi, 2\varphi_1, 2\varphi_2]$$

Those design variables with values out of grindable range will be physically meaningless. In other words, design for manufacturing has been taken into consideration.^[10] Therefore, the constraints on the design variables were determined based on the feasibility of the point grinding operation and are listed in Table 1.

4.2 Search Algorithm

Optimization of the MFD point geometry is based on the developed force models, which are not only nonlinear but also transcendental. Most search algorithms are difficult to apply due to the complexity of the force models. Also, optimization of the crankshaft MFD is a constrained optimization problem because design constraints are imposed on it. Therefore, a univariate exhaustive search technique was modified by imposing constraints in the searching process.

This search algorithm was performed by changing only one variable at a time until a minimal objective function, J , in said direction was found or until the constraint was reached. The search was continued until no further improvement could be made. The search began at a starting point and with the prescribed step size, $\alpha^i > 0$, in each of the coordinate directions, x_i , $i = 1, 2, \dots, n$. The algorithm is described as follows:

Initialize: set $K = 0$, X^0 and α^i , $i = 1, \dots, n$ are given. Given a starting base, x^k , find a temporary point, x^{k+1} , by the following process:

$$\begin{aligned} &\min \left[J(x_1^k, \dots, x_n^k), J(x_1^k \pm \alpha^1, x_2^k, \dots, x_n^k) \right] \\ &\min \left[\min \text{ of step}(r-1), J(\hat{x}_1^{k+1}, \dots, \hat{x}_{r-1}^{k+1}, x_r^k \pm \alpha^r, \dots, x_n^k) \right] \\ &\min \left[\min \text{ of step}(n-1), J(\hat{x}_1^{k+1}, \dots, \hat{x}_{n-1}^{k+1}, x_n^k \pm \alpha^n) \right] \end{aligned}$$

The point arrived at, \hat{x}^{k+1} , was used as a new base point, and the whole procedure started over again. This procedure was ap-

plied repeatedly until there was no significant improvement in the objective function in all searching directions. Also, in every step, the constraints were checked so that the search was executed in the constrained domain.

4.3 Optimization Results

The following three sets of initial values were used:

$$2\rho_{10} = \begin{bmatrix} 61^\circ \\ 91^\circ \\ 121^\circ \end{bmatrix} \quad 2\rho_0 = \begin{bmatrix} 75^\circ \\ 105^\circ \\ 135^\circ \end{bmatrix} \quad 2\rho_{20} = \begin{bmatrix} 89^\circ \\ 119^\circ \\ 149^\circ \end{bmatrix}$$

Note that the three different sets of initial values started from different regions of the constrained domain. The extrema searched were compared, and the one with the least objective function value was considered to be optimum.

Determination of the step size depends on the resolution of the drill grinder, which is 1° . Hence, the step size for all the three design variables was limited to 1° .

The search operation stopped when improvement of the objective function was less than 1% in all three searching directions. The optimum drill geometry searched is as follows:

$$2\rho_1 = 60^\circ$$

$$2\rho = 117^\circ$$

$$2\rho_2 = 150^\circ$$

5. Experimental Setup and Results

The split-point drill, the heuristic MFD, and the optimum MFD were all ground by a specially designed drill grinder. All of the drills used were of 0.25 in. (6.35 mm) diameter. The ground drills are shown in Fig. 6, and their geometric parameters are listed in Table 2. Tests were run to compare their thrust, torque, and drill life.

A radial drilling machine was used to drill workpieces, cut off from nodular cast iron crankshafts. A Kistler Type 9273 Dynamometer was used to measure thrust and torque. All of the measured signals were amplified by the Kistler Model 5004 Dual Mode Amplifier and then recorded onto a cassette tape with a TEAC R-81 Cassette Data Recorder. A Nicolet Model L206 Oscilloscope was used to monitor the measurements after the signals had been filtered by a low-pass filter. The spindle speed was 2100 rpm, and the feedrate was 0.007 ipr (0.178 mm/rev). The experimental setup is shown in Fig. 7.

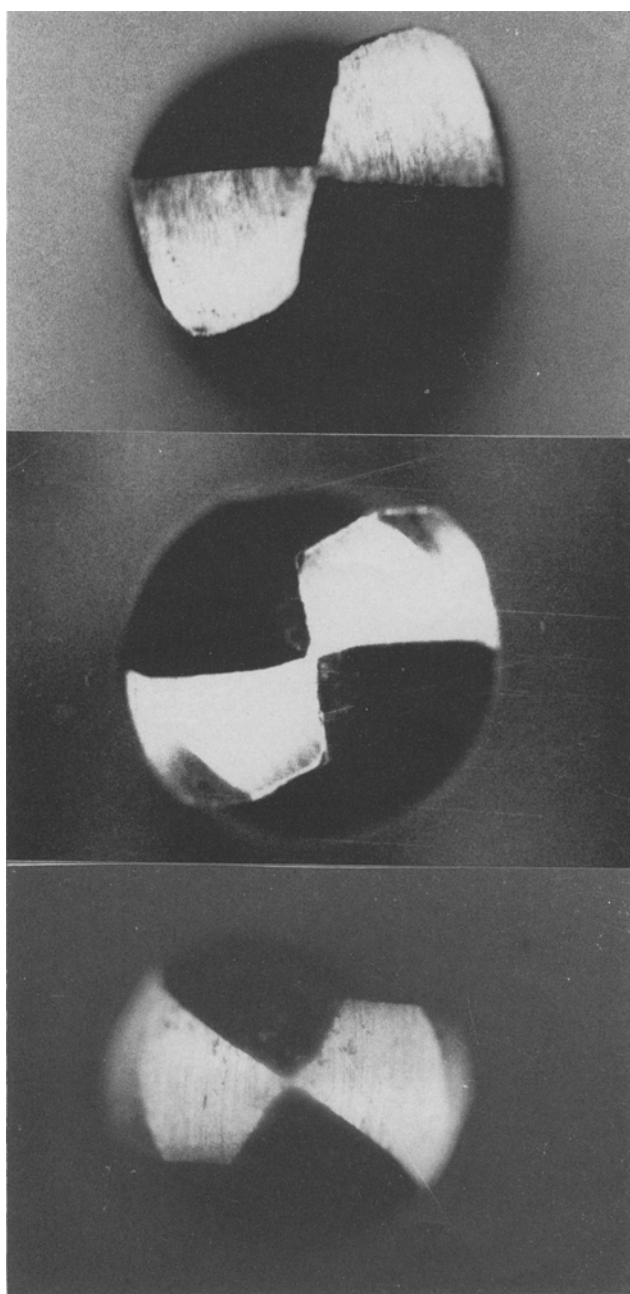


Fig. 6 (a) Split-point drill. (b) Heuristic MFD. (c) Optimum MFD.

Table 2 Geometric parameters of different type drills

Geometric parameters:	b , in. (mm)	l_2 , in. (mm)	2ρ	$2\rho_1$	$2\rho_2$	ψ	τ
Split-point drill	0.005 (0.127)	...	120°	...	150°	80°	58°
Heuristic MFD	0.005 (0.127)	0.020 (0.508)	120°	90°	150°	80°	58°
Optimum MFD	0.005 (0.127)	0.020 (0.508)	117°	60°	150°	80°	58°

Note: Chisel edge length, b ; length of the additional facet, l_2 ; point angles, 2ρ , $2\rho_1$, $2\rho_2$; chisel edge angle, ψ ; inner cutting edge angle, τ .

The measured thrust and torque of the heuristic MFD were 210.2 lb (935 N) and 28.9 lb · in. (326 N · cm), respectively. For the optimum MFD, the thrust was 165.5 lb (736 N) and the torque was 27.9 lb · in. (315 N · cm).

Compared to the heuristic MFD, the optimum MFD thrust is 21.3% less, whereas the torque decreased slightly, as shown in Table 3.

A radial drilling machine was used to drill 4.24×0.25 in. (107.70×6.35 mm) oil holes in nodular cast iron crankshafts. The crankshaft was held tightly by a drill rig, which had two drill bushings on it for oil hole drilling. The test setup is shown in Fig. 8.

Accelerated life tests were carried out to compare the performances of three different kinds of drills for crankshafts. During the tests, the spindle speed was 2100 rpm and the feed-rate was 0.007 ipr (0.178 mm/rev). When the drilling operations becomes very noisy, the drill is considered to be worn out. This drill life criterion is widely used in industry.

Under these conditions, the heuristic MFD produced three and four oilholes in two different tests; the optimum MFD produced five and six oil holes, respectively. The optimum MFD can increase drill life by 25% over the heuristic MFD. The experimental results are given in Table 4.

6. Conclusions

A two-stage design approach was used to develop an optimum MFD. A heuristic approach was used in the first stage, and computer-aided optimization were adopted in the second stage. The results of this design approach were successful.

A MFD has been heuristically developed in the first design stage that reduced thrust by 21.0% over a conventional split-point drill and increased drill life by 50% under accelerated life test conditions.

Force models for the MFD based on cutting mechanics have been developed. The computer-estimated thrust and torque values are within 20% of those obtained from experiments. To improve the performance of the heuristic MFD, an optimization program based on the force models was implemented to develop an optimum MFD in the second design stage. The results show that thrust and torque are further reduced by 21.3% and 3.5%, respectively. Accelerated life tests showed a 25% further increase in drill life.

Table 3 Thrust and torque of different type drills for crankshafts

Drills	Thrust, lb (N)	Torque, lb · in. (N · cm)
Split-point drill.....	266.1 (1184)	30.1 (340)
Heuristic MFD.....	210.2 (935)	28.9 (326)
Optimum MFD.....	165.5 (736)	27.9 (315)

Note: Spindle speed, 2100 rpm; feedrate, 0.007 ipr (0.178 mm/rev).

Table 4 Drill life of different type drills

Drills	No. of oil holes drilled	
	Test 1	Test 2
Split-point drill.....	2	2
Heuristic MFD.....	3	4
Optimum MFD.....	5	6

Note: Spindle speed, 2100 rpm; feedrate, 0.007 ipr (0.178 mm/rev).

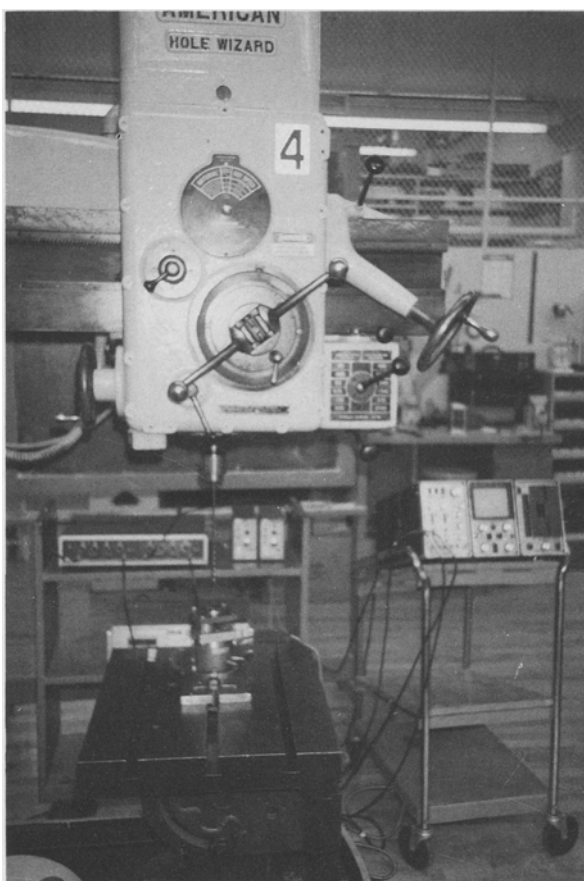


Fig. 7 Experimental setup for thrust and torque measurements.

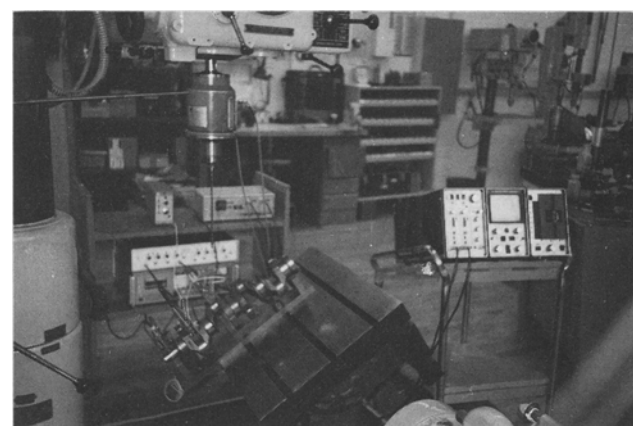


Fig. 8 Experimental setup for drill life tests.

Acknowledgment

This project is partially supported by NSF Grant No. DMC-8503405.

References

1. L.H. Chen and S.M. Wu, *ASME J. Eng. Ind.*, Vol 106, 1984, p 313-324
2. K.H. Fuh, Ph.D. thesis, University of Wisconsin-Madison, 1986
3. J.W. Lee, Ph.D. thesis, University of Wisconsin-Madison, 1986
4. S.M. Wu and J.M. Shen, *ASME J. Eng. Ind.*, Vol 105, 1983, p 173-182
5. T.I. Liu, *ASM J. Mater. Shap. Technol.*, Vol 9 (No. 3), 1991, p 161-169
6. J.M. Shen, L.H. Chen, and S.M. Wu, *Proc. 14th SAMPE, Material & Process Advances*, Vol 14, Atlanta, Oct 1982, p 464
7. R.A. Williams, *ASME J. Eng. Ind.*, Nov 1974, p 1207-1215
8. G.C.I. Lin and P.L.B. Oxley, *Proc. Inst. Mechan. Eng.*, Vol 186, 1972, p 813-820
9. I. Finnie and M.C. Shaw, *ASME Trans.*, Vol 78, 1956, p 1649-1657
10. T.I. Liu, *J. Concurrent Eng.*, Vol 1 (No. 3), 1991, p 12-19
11. P.L.B. Oxley, *Ann. CIRP*, Vol 13, 1966, p 128-138
12. M.G. Stevenson and P.L.B. Oxley, *Int. Proc. Inst. Mechan. Eng.*, Vol 184, 1970, p 561-576
13. S. Wiriayacosol and E.J.A. Armarego, *Ann. CIRP*, Vol 28/1, 1979, p 87-91
14. R.A. Venkataraman and F. Koenigsberger, Department of Machine Tool Engineering, the University of Manchester Institute of Science and Technology, 1975
15. A.R. Watson, *Int. J. Machine Tool Design Res.*, Vol 25 (No. 4), 1985, p 347-365